

Electrochemical Corrosion Tests in Low-Conductivity Ethanol–Gasoline Blends: Application of Supporting Electrolyte for Contaminated E5 and E10 Fuels

Lukáš Matějovský, Martin Staš,* and Jan Macák



Cite This: *ACS Omega* 2021, 6, 17698–17708



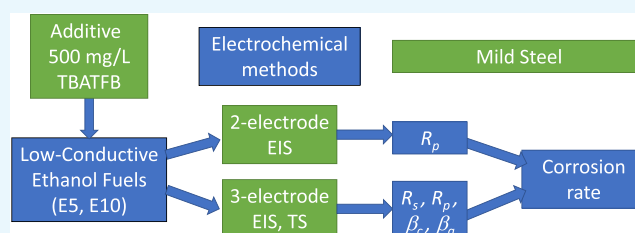
Read Online

ACCESS |

Metrics & More

Article Recommendations

ABSTRACT: Ethanol-based E5 and E10 fuels have extensively been used as automotive fuels in gasoline engines. However, especially when contaminated, these fuels can exhibit corrosion effects on some engine construction parts such as mild steel. Thus, the study of mild steel corrosion resistance has become of the utmost importance. Electrochemical methods such as electrochemical impedance spectroscopy (EIS) and polarization characteristics measurements (Tafel scan—TS) were proven to be very valuable in studying the mild steel corrosion behavior in ethanol–gasoline blends (EGBs). However, the use of these methods was, so far, very limited for low-ethanol-content EGBs such as E5 and E10 due to their low conductivity. In this study, we present modified EIS and TS corrosion measurements based on the use of tetrabutylammonium tetrafluoroborate (TBATFB) at 500 mg/L as a supporting electrolyte. This modification led to an increase in the contaminated E5 and E10 fuels' conductivity, which allowed us to successfully perform the electrochemical corrosion tests. The corrosion current densities were determined to be 1.5×10^{-3} and $1.5 \times 10^{-2} \mu\text{A}/\text{cm}^2$ for the tested E5 and E10 fuels, respectively. These modified methods present a significant extension of an electrochemical testing apparatus for steel corrosion studies in EGBs. They can allow one to obtain instantaneous information about the occurring corrosion process and, thus, estimate the materials' lifetime in corrosive environments and potentially help to prevent corrosion.



1. INTRODUCTION

The energy demands of mankind are growing year by year. Currently, fossil fuels are the most widespread energy source covering about 80% of the overall energy consumption.¹ However, the use of fossil fuels is associated with adverse environmental effects, such as an increasing level of carbon dioxide concentration in the atmosphere and the resulting global warming. Also, the stocks of fossil fuels are gradually decreasing. Thus, the importance of nonfossil, renewable energy sources (fuels) has increased dramatically especially in the last two decades.¹

Among the many potential renewable fuels, bioethanol is supposed to be the one with the highest potential to be directly applicable as a gasoline engine biofuel in transportation. Bioethanol can be used in a pure form (E100 fuel) or as a mixture with gasolines in so-called ethanol–gasoline blends (EGBs), which are designated as EX, where X defines the ethanol content in vol %.²

The biggest bioethanol producers are the United States and Brazil with the combined share of about 85% of the worldwide production.² Bioethanol can be produced by fermentation technology from different feedstocks containing simple or complex carbohydrates such as sugar beets, sugar cane, corn, wheat, maize, and potatoes. Bioethanol produced from these

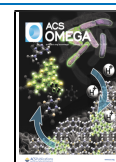
feedstocks, which are also applicable for food/feed production, is designated as a “first-generation biofuel.” The current trend leads to the use of biofuels of second and higher generations (advanced biofuels), which are produced from nonfood/feed biomass. The most important nonfood/feed bioethanol sources are different kinds of agricultural wastes with lignocellulosic characteristics.²

The physical and chemical properties of (bio)ethanol are significantly different from those of hydrocarbon-based petroleum fuels. Thus, the physical and chemical properties of EGBs obtained by the addition of (bio)ethanol into gasoline significantly differ from those of pure gasoline. The most problematic parameter of (bio)ethanol and EGBs intended to be used as a gasoline engine fuel is their corrosion effect on metallic materials in fuel systems. The study of corrosion effects of (bio)ethanol or EGBs on metallic materials is, thus, of the utmost importance.²

Received: May 3, 2021

Accepted: June 14, 2021

Published: June 25, 2021



Two main groups of methods have typically been used for corrosion studies of EGBs: gravimetric and electrochemical.³ The gravimetric methods evaluate the tested material weight change caused by corrosion processes. These methods are very simple and have very low instrumental requirements.³ However, the main disadvantage of these methods is the test duration, which is typically in the order of weeks or months. On the other hand, electrochemical methods have higher instrumental requirements than the gravimetric methods, but they can provide much more corrosion information including instantaneous corrosion data. The gravimetric and electrochemical methods have also been used to evaluate the efficiency of corrosion inhibitors. Based on these studies, substances such as ethanolamines, diethylenetriamine, hexamethylene triamine, piperazine, morpholine, and others were found to be promising steel corrosion inhibitors in ethanol environments.^{4–7} Electrochemical impedance spectroscopy (EIS) and polarization characteristics measurements (Tafel scan—TS) are the most typical methods for electrochemical corrosion studies of EGBs.^{3,4,8–11}

EIS and TS measurements in EGBs have typically been performed on fuels with a higher ethanol content, typically E85 and higher, as the conductivity of such fuels is high enough to obtain electrochemical corrosion data.^{4,8,10–27} Based on our own experience, we can conclude that EIS and TS measurements are generally not problematic for EGBs with an ethanol content of 40 vol % and more (E40 and higher). Overall, EIS can be performed in a two- or three-electrode arrangement, while TS can only be measured in three-electrode systems.

Two-electrode arrangements are generally more suitable for low-conductivity fuels as they are, unlike three-electrode arrangements, typically much less affected by parasitic elements and/or signal noise. Two-electrode arrangements make it possible to measure the polarization resistance even for EGBs with an ethanol content lower than 40% (E40 and lower). For E40, E25, and E20 fuels, the conductivity is typically still enough to obtain corrosion data when using a two-electrode measurement. For instance, Baena et al.⁵ successfully performed electrochemical measurements in a two-electrode measurement for E20 fuel. However, two-electrode measurements were typically still impossible to perform for E10 and lower fuels due to their very low (insufficient) conductivity.^{10,11}

Three-electrode arrangements are generally more informative than two-electrode measurements. This is associated with the fact that polarization characteristics (TS) can only be measured in this (three-electrode) arrangement.^{5,6,10,11} For EGBs lower than E40, the EIS spectra in a three-electrode arrangement can only be measured at high frequencies; hence, it is not possible to evaluate the polarization resistance, but only the environment information can be obtained. For the E5 and E10 fuels, neither information about the polarization resistance nor the environment information is typically obtainable when using a three-electrode measurement.^{10,11} Joseph et al.^{24,28} successfully performed polarization measurements in a three-electrode arrangement for steel in E20 fuel without any supporting electrolyte.

From the above-mentioned text, it follows that the electrochemical measurements in EGBs become much more difficult with a decreasing ethanol content resulting in a decreasing conductivity, which is valid especially for three-electrode measurements. Typically, three-electrode measurements do not allow one to reliably obtain electrochemical

corrosion data for EGBs lower than E40. Conversely, two-electrode measurements can be performed even in E10 fuels, but very long exposure times (more than 24 h) are needed so instantaneous corrosion information cannot be obtained for such (and less conductive) fuels.^{9–11} Thus, electrochemical measurements in (bio)fuels with a very low conductivity are very limited and the gravimetric methods are often the only option to obtain corrosion data about such fuels.^{9–11}

The basic problem of the electrochemical methods' application for corrosion studies in low-conductivity (bio)fuels is the high resistivity of such (bio)fuels. Those who conduct electrochemistry in aprotic environments usually solve this problem by using base (supporting) electrolytes (e.g., tetraalkylammonium tetrafluoroborates, perchlorates, etc.), which are soluble in the used environments and increase the environment conductivity.^{20,29} This solution is not always optimal in the case of corrosion studies as the supporting electrolytes are generally surfactants, affect the corrosion rate, and may have inhibitory abilities.²⁰ Thus, the use of supporting electrolytes may, in some cases, result in a significant distortion of the obtained results.²⁰ Due to the low conductivity of the environment, the *iR*-drop (potential loss due to the resistivity of the environment) can be high and the measurements can be associated with many problems. Cao et al.³⁰ tested several supporting electrolytes in corrosion cracking of steel in an ethanol (ASTM D4806) environment using cyclic potentiodynamic polarization. The influence of the individual supporting electrolytes (lithium perchlorate, lithium chloride, and lithium nitrate, 1-ethyl-3-methyl-imidazolium tetrafluoroborate, tetrabutylammonium hexafluorophosphate, tetraethylammonium tetrafluoroborate, and tetrabutylammonium tetrafluoroborate (TBATFB)) was studied. TBATFB at a concentration of 0.01 M was shown to have the lowest effect on the bias.^{21,30} Some other studies mention the use of sodium and lithium perchlorates as supporting electrolytes in EGBs with a higher ethanol content.^{6,29} However, it was shown that lithium perchlorate was inappropriate for corrosion cracking testing.²⁹ In EGBs, lithium perchlorate facilitated steel passivation and, thus, negatively affected data obtained during corrosion cracking.²⁹ In our previous study, we showed that at a relatively low concentration of 100 mg/L, lithium perchlorate can be used for EIS measurements. However, higher concentrations of this electrolyte (~500 mg/L) can negatively influence impedance measurements. At the lithium perchlorate concentration of 500 mg/L, the EIS low-frequency part was adversely affected. This spectrum part consisted of two time constants, which made the spectrum and its interpretation more complicated.⁹

As mentioned above, the corrosion testing of E5 and E10 fuels was, so far, almost solely limited to the use of gravimetric methods. Although these methods are reliable, reproducible, and very simple, they do not provide instantaneous corrosion information since testing periods are in the order of weeks or months. So far, corrosion data were impossible to be obtained for E5 and E10 fuels by EIS or TS measurements due to the very low conductivity of these fuels.

TBATFB was solely used as a supporting electrolyte in fuels with a high ethanol content so far. These environments exhibit relatively high electrolytic properties.^{10,11} Measurements in these environments can be performed without supporting electrolytes. To our best knowledge, the use of TBATFB has not yet been reported in low-ethanol-content fuels such as E10 and lower. These environments exhibit low electrolytic

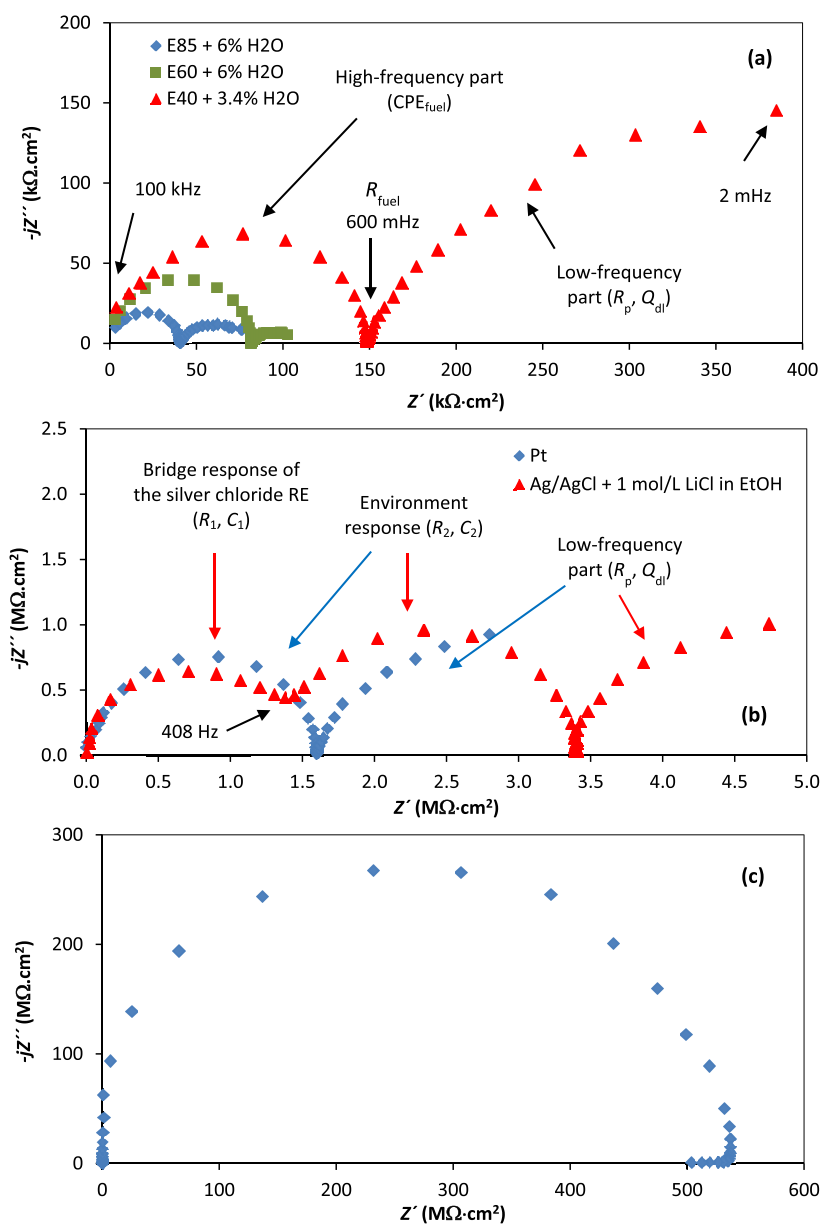


Figure 1. EIS spectra of mild steel measured in the three-electrode arrangement in the contaminated EGBs: (a) fuels with a higher ethanol content and sufficient conductivity, (b) impedance in the contaminated E10 fuel after the TBATFB addition, and (c) impedance in the contaminated E5 fuel after the TBATFB addition using a reference platinum electrode.

properties and have significantly different behavior compared with fuels with higher ethanol contents. Electrochemical measurements in low-ethanol-content fuels such as E5 and E10 cannot be performed in three-electrode arrangements.

1.1. Goal of the Study. This paper follows our previous studies aimed at developing methods for electrochemical corrosion studies in EGBs with a very low conductivity such as E10 and E5 fuels.^{3,9} Our strategy was to use supporting electrolytes to increase the conductivity of such fuels to values that would be high enough for electrochemical corrosion measurements. In a previous study by Matějovský et al.,⁹ the testing of potentially suitable supporting electrolytes for such corrosion studies was performed and TBATFB at 500 mg/L was chosen as a suitable supporting electrolyte for further testing.

In this study, we present the modification of the EIS and TS measurement methods currently available to the corrosion

studies of EGBs higher than E10. The modification is based on the use of TBATFB at 500 mg/L as a supporting electrolyte. The testing was performed in originally very low conductive fuels E5 and E10. TBATFB was found to increase the conductivity of the contaminated E5 and E10 fuels to obtain measurable values by the above-mentioned methods. Also, the data distortion caused by the supporting electrolyte was found to be negligible. This method represents a significant extension of the corrosion testing apparatus for E5 and E10 fuels.

2. RESULTS AND DISCUSSION

2.1. Sample Selection. Mild steel was selected as the most widespread construction material in car fuel lines and different transportation, storage, and production facilities that can come into contact with pure ethanol (E100) or EGBs. As an example of the corrosion environment, E5, E10, E40, E60, and E85 fuels (EGBs) were selected. E5, E10, and E85 fuels are

commercially available while E40 and E60 fuels are not. However, E40 and E60 (and other) blends can be formed in fuel tanks of so-called flexible-fuel vehicles (allowing for the burning of EGBs with any ratio of ethanol and gasoline), when refueling such cars with EGBs with different ethanol contents. The range of EGBs was chosen to evenly cover a wide range of ethanol content in fuels. In the E40, E60, and E85 fuels, the corrosion information can be obtained without a supporting electrolyte. This information is important to compare the results obtained in the low-conductivity E5 and E10 fuels doped with a supporting electrolyte.

2.2. Three-Electrode Arrangement—EIS and TS. The three-electrode system used in this study consisted of a mild steel working electrode, a platinum wire auxiliary electrode, and a platinum microelectrode serving as a pseudo-reference electrode (see Section 4.3.1). The platinum potential is dependent on the oxygen solubility in an environment. The oxygen solubility changes depending on the ethanol content in the EGBs. For this reason, the potential of the working electrode was always measured against the potential of the full-featured silver chloride reference electrode before each EIS and TS measurement. Instead of a frit, the silver chloride electrode uses a conductive connection via a ground joint. After the potential measurements, this electrode was always removed from the electrochemical cell to prevent any chloride leakage from the ground joint of the electrode bridge. The advantage of the platinum pseudo-reference electrode was the elimination of parasitic elements appearing at high frequencies of the impedance spectra. As presented above, these parasitic elements are related to the cell geometry and the bridge response of the reference silver chloride electrode.

2.2.1. Three-Electrode EIS. The comparison of the mild steel EIS spectra measured in the three-electrode arrangement in the different contaminated fuels is presented in Figure 1. These spectra can be interpreted using the equivalent circuits presented in Figure 2. The evaluated parameters from these spectra using the equivalent circuits are presented in Tables 1 and 2.

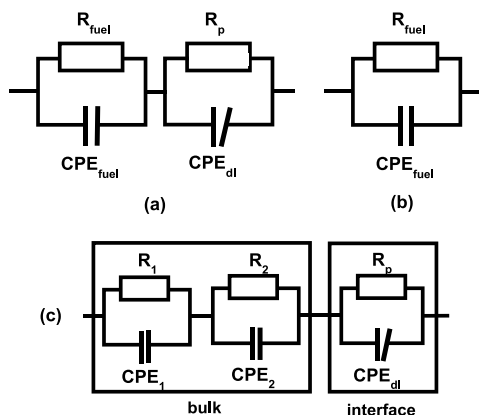


Figure 2. Equivalent circuits used for the approximation of the EIS spectra in Figure 1: (a) the circuit corresponding to the transmission response of the environment and the electrode interface, (b) the circuit corresponding to the spatial environment impedance only, (c) the circuit corresponding to the response of the (i) environment, (ii) salt bridge Ag/AgCl of the RE, and (iii) electrode interface. Adapted with permission from refs 411. Copyright 2018 and 2019 American Chemical Society.

The EIS spectra presented in Figure 1 have, in all cases, in the complex plane, the shape of one, two, or three half circles centered below the real axis. The evaluation of the half circles of the EIS spectra was performed by the approximation using a parallelly connected resistor and a constant phase element (CPE). This approximation can be expressed by eq 1

$$Z = \frac{R}{1 + RQ(j\omega)^n} \quad (1)$$

where R is the parallel resistor, Q is the CPE coefficient, n is the CPE exponent, ω is the angular frequency, and j is the imaginary unit. The interpretation of R and Q mainly depends on the type of the corrosive environment and whether it is the high-frequency or low-frequency spectrum part.

Ethanol, due to its relatively high polarity ($\epsilon_r = 24$), does not exhibit a high environment resistance, and its conductivity is sufficiently high enough to perform electrochemical measurements. Conversely, nonpolar types of gasoline ($\epsilon_r = 2-3$) typically have very low conductivity. The polarity of EGBs contaminated by water ($\epsilon_r = 78$) and salts is strongly influenced by the content of these contaminants. Naturally, the EGBs' polarity increases with the increasing water, ion, and ethanol contents. Thus, such high-conductivity fuels act more like an electrolyte. In this case, the EIS spectra of mild steel–fuel (E40 and higher) systems measured in a three-electrode arrangement using a platinum pseudo-reference electrode had a shape of two relatively well-separated half circles. In such environments (fuels), the electrolytic properties are exhibited and no other additional (supporting) electrolyte is necessary. For E10 fuels with no supporting electrolyte, the EIS spectra typically consist of one half circle that corresponds to a high-frequency response (see Figure 1c). From this half circle, only the environment (fuel) response, but no information about the tested materials, can be obtained. For E5 fuels with no supporting electrolyte, typically no information about the tested materials or fuels can be obtained when a three-electrode system is used.

A similar spectrum shape was measured in the E10 fuel after the addition of TBATFB in a three-electrode system with a platinum pseudo-reference electrode, as shown in Figure 1b (the blue spectrum). All these spectra are formed by high- and low-frequency loops corresponding to the equivalent circuit shown in Figure 2a. The parameters of these EIS spectra are compared in Table 2. The high-frequency part of the spectra is associated with the impedance response of the environment (the so-called spatial impedance).

From this part, one can evaluate the series resistance R_s and Q (from eq 1) value that is associated with the environment conductivity and polarity. The C_{eff} value presented in Tables 1 and 2 can be calculated from these values from eq 2.

$$C_{\text{eff}} = Q^{1/n} \cdot R^{(1-n)/n} \quad (2)$$

Since the n values for high-frequency CPE are close to 1, then the C_{eff} values are very close to Q . The high-frequency capacitances C presented in Table 1 are directly proportional to the relative environment permittivity, which increases depending on the increasing content of ethanol, water, ions, and TBATFB in the fuel.

The low-frequency impedance loop in Figure 1a,b is related to the response of the electrical double layer at the phase interface and the polarization resistance of the mild steel. The polarization resistance is an important basic corrosion variable

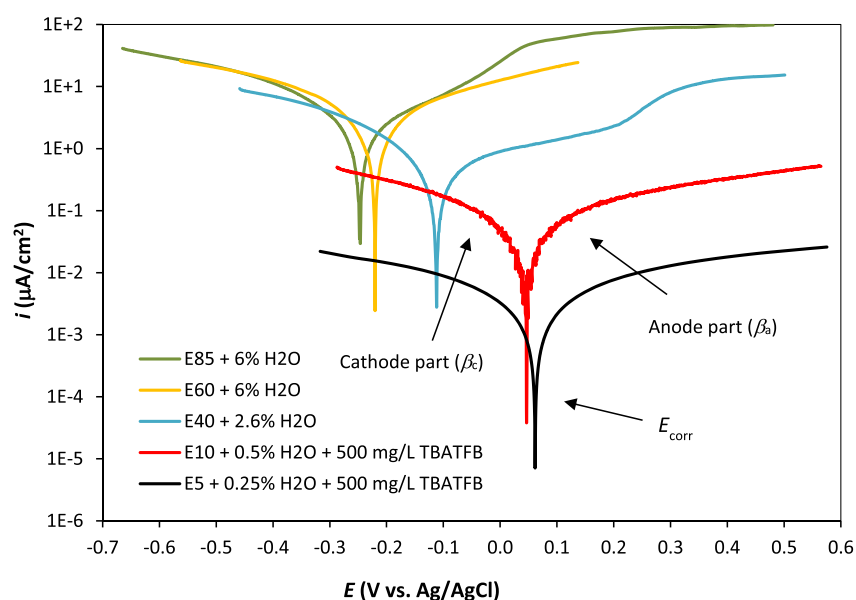
Table 1. Parameters of the EIS Spectra of the Mild Steel in Figure 1 Evaluated by Approximation Using the Equivalent Circuit and Recalculated to the Surface Area of the WE

fuel	high-frequency impedance		low-frequency impedance		
	R_s ($k\Omega \text{ cm}^2$)	C (nF/cm^2)	R_p ($k\Omega \text{ cm}^2$)	Q_{dl} ($\mu\Omega^{-1} \text{ s}^n/cm^2$)	n
E85 + 6 vol % H_2O	40.5	0.487	42.7	11.1	0.6972
E60 + 6 vol % H_2O	81.0	0.386	25.5	30.0	0.6271
E40 + 2.6 vol % H_2O	167	0.199	467	72.4	0.6888
E10 + 0.5 vol % H_2O	59 700	0.007	-	-	-
E10 + 0.5 vol % H_2O + TBATFB	1560	0.359	2315	26.9	0.8699
E5 + 0.25 vol % H_2O + TBATFB	108 300	0.008	-	-	-

Table 2. Parameters of the Mild Steel EIS Spectra Measured in the E10 Fuel Containing 0.5 vol % of Water after Adding TBATFB^a

RE	high-frequency impedance				low-frequency impedance		
	R_1 ($k\Omega \text{ cm}^2$)	C_1 (nF/cm^2)	R_2 ($k\Omega \text{ cm}^2$)	C_2 (nF/cm^2)	R_p ($k\Omega \text{ cm}^2$)	Q_{dl} ($\mu\Omega^{-1} \cdot \text{s}^n/cm^2$)	n
Pt	1 560	0.359	-	-	2 315	26.9	0.8699
Ag/AgCl	1 420	0.047	2 105	2.71	2 362	27.7	0.8723

^aThe three-electrode arrangement with platinum RE and silver chloride WE with a bridge; the values are recalculated to the WE surface area.

**Figure 3.** Tafel polarization curves of the mild steel in the contaminated EGBs measured after 24 h of exposure.

that is inversely proportional to the corrosion rate. Using the Stern–Geary equation and polarization characteristics, the polarization resistance can be converted to the corrosion current density that is directly proportional to the corrosion rate.

If the full-featured reference electrode was used instead of the pseudo-reference electrode, the spectrum in the high-frequency area was formed by two time-constants, as demonstrated in Figure 1b (the red spectrum). The presence of this time constant is caused by the response of the salt bridge of the full-featured reference silver chloride electrode. The second time constant in the frequency range of 408 Hz to 600 mHz refers to the environment response. This spectrum can be interpreted using the equivalent circuit presented in Figure 2c. The parameters of the impedance spectra are shown in Table 2.

The impedance spectrum shown in Figure 1c was measured at the highest used amplitude of the perturbation signal (50 mV) in the contaminated E5 fuel containing 500 mg/L of

TBATFB. The low polarity of the E5 environment leads to the absence of the formation of an electric double layer, and the spectrum is, thus, formed by a single half circle starting from the beginning of the complex plane with the end lying on the real x -axis. The equivalent circuit corresponding to this spectrum is presented in Figure 2b. The R and Q elements must be interpreted as the environment resistance and the ideal environment capacitance. From these values, only the information related to the fuel (resistivity and permittivity) can, thus, be obtained; the material corrosion based on the electrical double-layer capacitance and polarization resistance cannot be evaluated. A similar spectrum consisting of a single half circle with no response in the low-frequency area was obtained using EIS in the contaminated E10 fuel without the supporting electrolyte TBATFB also (see the spectrum parameters in Table 1).

From Table 1, it follows that the series resistance R_s of the environment decreased depending on the ethanol content in the EGBs and their contamination. This series resistance

Table 3. Parameters Evaluated from the Polarization Curves (Figure 3) and the Calculated Corrosion Current Densities of the Mild Steel from eq 3 (Based on R_p in Table 1)

fuel	β_c (V/dec)	β_a (V/dec)	E_{corr} (mV vs Ag/AgCl)	i_{corr} ($\mu\text{A}/\text{cm}^2$)
E85 + 6 vol % H_2O	0.20	0.20	-248	1.1
E60 + 6 vol % H_2O	0.35	0.39	-220	3.2
E40 + 2.6 vol % H_2O	0.14	0.50	-114	0.1
E10 + 0.5 vol % H_2O + TBATFB	0.14	0.20	48	0.015
E5 + 0.25 vol % H_2O + TBATFB	0.23	0.21	61	1.5×10^{-3a}

^aThe mild steel corrosion density calculated based on the polarization resistance evaluated from the polarization curve.

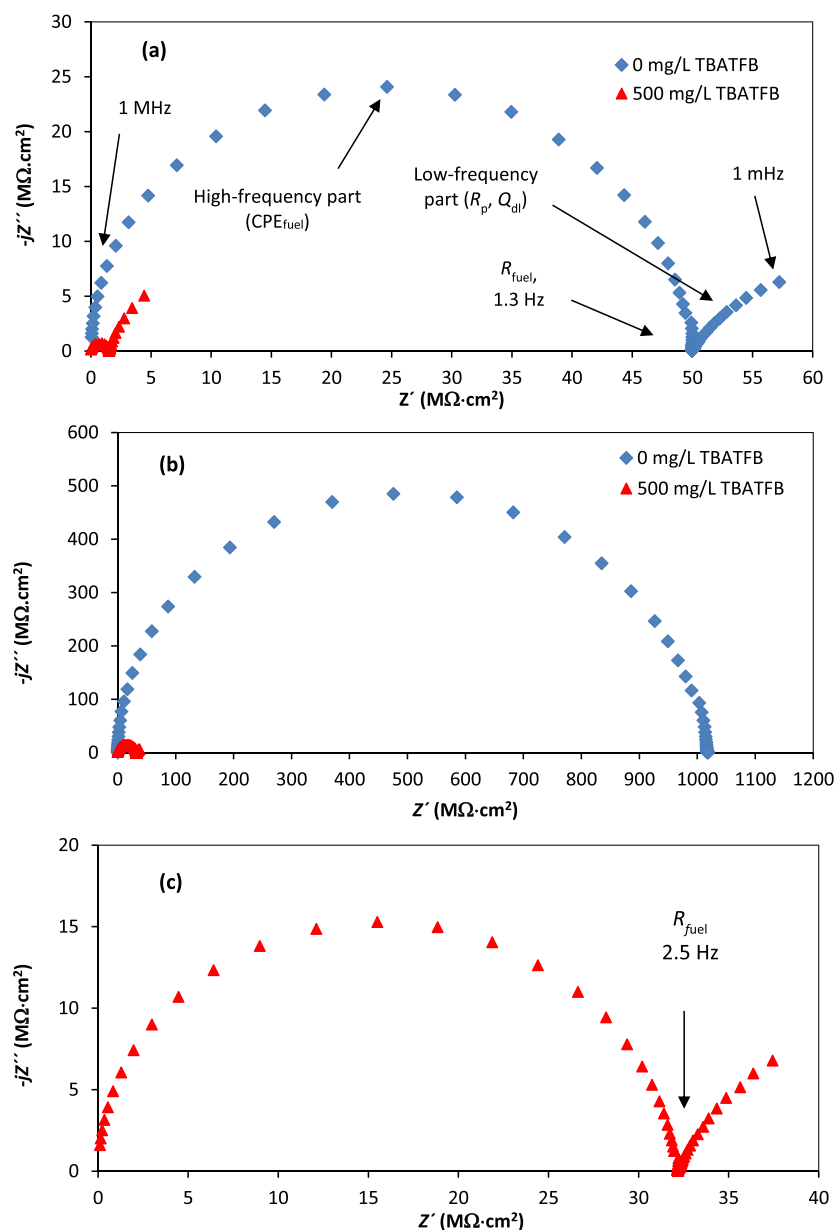


Figure 4. Comparison of the mild steel EIS spectra after 24 h of exposure measured in the contaminated E5 and E10 fuels in the two-electrode arrangement with and without the supporting electrolyte (TBATFB): (a) E10, (b) E5, and (c) the zoomed-in EIS spectrum measured in the E5 fuel after addition with the supporting electrolyte from (b).

significantly decreased after the addition of TBATFB as documented by the comparison of the R_s values before and after the addition. This is also related to the increase in capacitance in the high-frequency area. The environment becomes more conductive and behaves more like an electrolyte. As the ethanol content in the fuel decreases, the

mild steel polarization resistance rises by 1 order of magnitude. This increase in the polarization resistance refers to the decrease in the mild steel instantaneous corrosion rate. The only exception is the contaminated E60 fuel in which the mild steel showed the lowest R_p values. This result confirms the results published in our previous studies where we showed that

Table 4. Mild Steel EIS Spectra Parameters Measured in the Two-Electrode Arrangement (Figure 4) and Recalculated to the Total Surface Area

fuel	TBATFB 500 mg/L	E_{corr} (mV)	high-frequency impedance		low-frequency impedance		
			R_s ($M\Omega \text{ cm}^2$)	C (pF/cm 2)	R_p ($M\Omega \text{ cm}^2$)	Q_{dl} ($\mu\Omega^{-1} \text{ s}^n/\text{cm}^2$)	n
E5 + 0.25 vol % H $_2$ O	no	−6.8	1007	1.12	-	-	-
	yes	−6.1	32.1	1.20	24.3	5.27	0.7830
E10 + 0.5 vol % H $_2$ O	no	−9.7	49.8	1.41	16.4	4.41	0.7832
	yes	−9.4	1.50	1.56	15.9	6.36	0.8141

the E60 fuel after the contamination or oxidation was the most corrosively aggressive fuel among all the EGBs tested.^{4,10,11} The mild steel polarization resistance presented in Table 2 obtained for the E10 fuel showed very good agreement, and the standard deviation of these measurements was lower than 5%.

After 23 h of open circuit potential (OCP) stabilization of the mild steel–E5 and mild steel–E10 systems, TBATFB was added directly into the system. After the dissolution of TBATFB in the systems and further OCP stabilization occurring for 15 min, any significant changes in the corrosion potential values were observed. The change in the corrosion potential was not higher than 5 mV. The addition of E5 and E10 fuels by the supporting TBATFB electrolyte significantly decreases the environment resistance by 2 orders of magnitude minimally, which makes it possible to measure the EIS spectra as well as the polarization curves in these low-conductivity EGBs.

2.2.2. Three-Electrode TS. Figure 3 shows the comparison of the mild steel polarization curves in the different EGBs after the iR -drop compensation. The polarization characteristics (E_{corr} , β_a , β_c) evaluated from these curves and the calculated (from the polarization resistances, see Tables 1 and 2, according to eq 3) relevant corrosion current densities i_{corr} of the mild steel are presented in Table 3.

Ideally, linear Tafel values are very rare for EGBs. The coefficient evaluation for the cathode and anode polarization curves (β_a , β_c) was performed from the areas of 50–200 mV toward E_{corr} . It should be noted that the Tafel constants affect the calculated corrosion current to a relatively small extent. Often, these values are not determined experimentally, but their value is chosen to calculate the current density. According to the evaluated values of β_a and β_c , which are reasonable in our opinion, we believe that these values will not be loaded by a significant error. Thus, the calculated corrosion current densities presented in Table 3 should not be loaded by an error either.

Since no response at low frequencies was measured in the contaminated E5 fuel containing 500 mg/L of TBATFB at the EIS measurements, it was not possible to evaluate the polarization resistance to calculate the corrosion current density according to eq 3. The polarization resistance (R_p) value was obtained from the course of the polarization curve. The polarization resistance value of the mild steel in the E5 fuel determined from the polarization curve was 31.4 $M\Omega \text{ cm}^2$. However, important information about the environment resistance for the iR -drop compensation was obtained from the EIS spectrum.

According to Figure 3 and Table 3, it is obvious that, depending on the ethanol content in the fuels, the polarization curves shift toward positive potentials and to the lower corrosion current densities that refer to lower instantaneous corrosion rates of the mild steel. The positive values of the

corrosion potential of the mild steel in the contaminated E5 and E10 fuels (see Table 3) show that the mild steel is in the potential area where steel is in a passive state. The very low corrosion rates of the mild steel and low corrosion aggressiveness of the contaminated E5 and E10 fuels correspond to this state as well. The results correspond to the assumption that the decreasing ethanol content decreases the aggressiveness of the EGBs. According to the literature, the contaminated E5 and E10 fuels do not show any significant decrease in the material compatibility with the mild steel. The obtained corrosion current densities of the mild steel in the E5 and E10 fuels, which are 2–3 orders of magnitude lower compared to the most aggressive E60 fuel, correspond to very low corrosion rates. This fact shows the meaningfulness of the measured data at the polarization and the EIS measurements using TBATFB in the three-electrode arrangement in the contaminated E5 and E10 fuels.

2.3. Two-Electrode Arrangement—EIS. The measured EIS spectra in the two-electrode arrangement for 24 h of exposure (see Figure 4) are like the spectra from the three-electrode arrangement (see Figure 1). In both these cases, the spectra had in the complex plane the shape of one or two relatively well-separated half circles centered below the real axis. These spectra can be interpreted using the equivalent circuits from Figure 2a,b. The evaluated parameters of the EIS spectra using the equivalent circuits are presented in Table 4.

Unlike the three-electrode arrangement (see Table 1), the two-electrode arrangement allowed us to measure the low-frequency loop without the supporting electrolyte (see Figure 4a and Table 4). Thus, it was possible to obtain information about the corrosion properties (Q_{dl} and R_p) of the mild steel. Thus, it is obvious that the cell geometry of the two-electrode system favorably contributes to the response at low frequencies, which can only be measured using sufficiently sensitive potentiostats. Another positive aspect was a sufficiently long exposure time that allowed the formation of an electric double layer on the phase interface of the mild steel–E10 fuel system. The capacitance of the double layer had values that were already measurable by using the analytical equipment. Without the formation of an electrical double layer on the mild steel–fuel interface, it is not possible to measure the impedance response at low frequencies as documented in Figure 4b for the contaminated E5 fuel. The spectrum corresponding to the contaminated E5 fuel shown in Figure 4b was formed only by a single half circle, which corresponded to the spatial impedance. The spatial impedance makes it possible to evaluate the ideal capacitance and environment resistance. In the two-electrode system, the contaminated E5 fuel acted less like an electrolyte in comparison with the contaminated E10 fuel. This is also documented by the significantly higher environmental resistance and slightly lower high-frequency capacitance (see Table 4). The conductivity increase achieved by the addition of TBATFB allowed us to

measure the response at low frequencies even for the contaminated E5 fuel (see Figure 4c).

The addition of the contaminated E5 and E10 fuels by TBATFB was performed similarly as in the case of the three-electrode arrangement. After the OCP stabilization for 23 h, TBATFB was added, and after a further 15 min, the EIS measurement was performed. The values of the corrosion potential before and after the addition of the supporting electrolyte are presented in Table 4. For both the fuels, the addition of the supporting electrolyte had no significant effect on the corrosion potential change and only a slight increase was observed. The addition of TBATFB at 500 mg/L led to a significant decrease (min. 30 times) in the environmental resistance in both cases.

The mild steel corrosion potentials presented in Table 4 are very positive, which indicates (i) the very low corrosivity of the E5 and E10 fuels and (ii) a very high mild steel corrosion resistance. This is also indicated by very high polarization resistances. The higher resistance of the mild steel in the E5 and E10 fuels is demonstrated either by a higher value of the corrosion potential or about one-third higher polarization resistance. The difference in the polarization resistance measured in the E10 fuel before and after the addition of TBATFB was lower than 5%. This difference illustrates a good level of repeatability and a low level of distortion of the information obtained due to the presence of TBATFB. This supporting electrolyte had a low impact on the electrode properties for the short-term exposures only. As the experiment time increases, the effect of TBATFB on the electrode properties may increase significantly due to the slow adsorption of TBATFB on the steel surface. TBATFB exhibits a slight inhibitory effect at longer exposures, which increases with the exposure time.⁹

The mild steel polarization resistance values from the two-electrode and the three-electrode arrangements cannot be compared as the ratio of the mild steel surface area versus the corrosion environment (fuel) volume was not maintained at the same level for both methods (see Table 1). Thus, only the trends depending on the ethanol content in the fuels after enough exposure periods can be compared. This is caused by the fact that the corrosion process course and its stabilization overtime vary with the different ethanol ratios. The amount of the dissolved oxygen in the system and its ratio to the electrode surface area can also influence the corrosion process course as oxygen is involved in the depolarization reactions. The amount of the dissolved oxygen in both fuels was not the same. The solubility of oxygen in water and ethanol is several times lower than in gasoline so that as the ethanol content increases, the dissolved oxygen content in the model fuel decreases. Nevertheless, both methods provide very valuable results and make it possible to measure in a very low conductive environment where the environment has almost no electrolyte properties.

3. CONCLUSIONS

In this study, we performed electrochemical measurements in a two-electrode (EIS) and three-electrode arrangement (EIS, TS) in the environment of low-conductivity E5 and E10 fuels on mild steel using TBATFB as a supporting electrolyte. We demonstrated that TBATFB at 500 mg/L decreases the environment resistance and allows one to, thus, obtain measurable corrosion data of the mild steel in the environment of the E5 and E10 fuels. For the E10 fuel, TBATFB allowed us

to obtain measurable EIS spectra with the response at low frequencies. From these spectra, it was possible to evaluate the polarization resistance that informed us about the corrosion rate. TBATFB in the E5 fuel made it possible to measure a spectrum with the environment response. This spectrum is important to evaluate the environment resistance, which is important for *iR*-drop compensation in the polarization measurements. TBATFB in the environment of the E5 and E10 fuels using a sufficiently sensitive potentiostat allows us to measure the polarization curves even in the areas of very low current densities. The polarization resistance in the environment of the E5 fuels can be evaluated from the course of the polarization curve. It was possible to determine the corrosion current density of the mild steel according to the Stern–Geary equation in the environment of both the fuels. The value of the corrosion current density of the mild steel was 1.5×10^{-3} and $1.5 \times 10^{-2} \mu\text{A}/\text{cm}^2$ for the contaminated E5 and E10 fuels, respectively.

The planar, two-electrode arrangement makes it possible, thanks to its cell geometry, to measure the EIS spectra with the response at low frequencies in the E5 fuel when using TBATFB. Thus, it is possible to evaluate the polarization resistance from the obtained impedance values. In the three-electrode arrangement, this is not possible even when using TBATFB as the supporting electrolyte.

For the two- and three-electrode arrangements, TBATFB did not influence the corrosion potential of the mild steel from a short-term point of view. The obtained resistance values, the position of the polarization curves, and the calculated values of the mild steel corrosion current densities indicate the meaningfulness of the obtained data and the high applicability of these measurement techniques using TBATFB in low ethanol fuel environments (E5 and E10).

4. EXPERIMENTAL SECTION

4.1. Preparation of EGBs. The EGBs used in this work (E5, E10, E40, E60, and E85) were prepared from a gasoline base and absolute ethanol (99%, pro analysi, Penta a.s., the Czech Republic) containing less than 700 mg/kg of water. The gasoline base was prepared by mixing different gasoline pool fractions with a low sulfur content: reformate, isomate, and light, middle, and heavy naphtha ($\text{C}_5\text{--C}_6$, $\text{C}_6\text{--C}_8$, and $\text{C}_8\text{--C}_{12}$, respectively) from fluid catalytic cracking. All the fractions were obtained from the Unipetrol refinery situated in Kralupy nad Vltavou (the Czech Republic). These fractions were mixed in such a ratio that the obtained gasoline base met the requirements of the EN 228 standard. The resulting group-type composition of the prepared gasoline base was determined by gas chromatography and was as follows: saturated hydrocarbons, 51.6 vol %; unsaturated hydrocarbons, 14.0 vol %; and aromatic hydrocarbons, 34.4 vol %.

Then, the total sulfur content was determined in the gasoline base according to ASTM D5453, and the obtained value was 2 mg/kg of sulfur, which meets the requirements of the EN 228 standard.

4.2. Contamination of EGBs. The electrochemical measurements were performed under simulated contamination. All of the tested fuels were purposely contaminated by a solution containing 875 mg/L of acetic acid, 51.7 mg/L of sulfuric acid, 53.3 mg/L of sodium chloride, and 45.0 mg/L of sodium sulfate. The composition of the contamination solution was chosen based on the literature data.^{6,10,11} The contamination level was chosen so that the ASTM D4806-13 standard

Table 5. Content of the Contamination Solution in the Tested Fuels, the Applied Electrochemical Methods with Their Electrode Arrangement, and the Ratio of the Working Electrode Surface Area vs the Fuel Volume^a

fuel	contamination solution					electrochem. methods	electrode arrangement (the number of electrodes)	WE surface area vs fuel volume (cm ² /cm ³)
	water (vol %)	Na ₂ SO ₄ (mg/L)	H ₂ SO ₄ (mg/L)	NaCl (mg/L)	CH ₃ COOH (mg/L)			
E85	6	2.7	3.1	3.2	52.5	OCP, EIS, TS	3	5/100
E60	6	2.7	3.1	3.2	52.5	OCP, EIS, TS	3	5/100
E40	2.6	1.2	1.3	1.4	22.8	OCP, EIS, TS	3	5/100
E10	0.5	0.23	0.26	0.27	4.4	OCP, EIS, TS	3	5/100
E5	0.25	0.11	0.13	0.13	2.2	OCP, EIS	2	24/100
						OCP, EIS, TS	3	5/100
						OCP, EIS	2	24/100

^aEIS, electrochemical impedance spectroscopy; OCP, open circuit potential; TS, Tafel scan; WE, working electrode.

requirements for fuel contamination were met. Therefore, a decreasing contaminant content in the EGBs was used depending on the decreasing ethanol content. The water content was chosen regarding the water solubility in the fuel and its possible real contamination. All of the chemicals used to prepare the contamination solution were of pro analysis purity and were dissolved in demineralized water. The amount of the contamination solution added into the tested fuels is specified in Table 5.⁹

4.3. Electrochemical Apparatus. Electrochemical measurements were performed in two- and three-electrode arrangements (see Table 5). The three-electrode arrangement was used for the contaminated E5, E10, E40, E60, and E85 fuels for the EIS and TS measurements, and the two-electrode arrangement was used for the same fuels for the EIS measurements only (TS was not performed).

The E40, E60, and E85 fuels with the relatively high conductivity (no addition by the supporting electrolyte) and the low-conductivity E5 and E10 fuels (after the addition) were analyzed by the EIS and TS measurements.

4.3.1. Three-Electrode Arrangement (EIS and TS). The measurements were performed in a 100 mL electrochemical cell. The electrode system consisted of working, auxiliary (counter), and reference electrodes (WE, CE, and RE, respectively). The WE was made of mild steel and had a cylindrical shape, and its surface area was 5 cm². A spiral from a platinum wire coaxially oriented to the WE was used as the AE. A platinum microelectrode was used as the pseudo-RE. This electrode consisted of a platinum wire insulated in a polytetrafluoroethylene tube. The distance between the WE and the noninsulated wire end of the RE was 1–2 mm. Before each EIS and TS measurements, the potential of the WE was measured against a full-featured silver chloride electrode (Metrohm) equipped with a salt bridge containing a 1 M solution of lithium chloride in ethanol.^{3,9}

All electrochemical measurements were performed in a grounded Faraday cage. The EIS and TS measurements were performed with Solartron 1250FRA and Solartron SI 1287 after the stabilization of the corrosion potential, which took 24 h. The impedance spectra were measured in the frequency range of 60 kHz to 2 mHz at an amplitude of 5–50 mV in dependence on the fuel conductivity (see Table 6). The amplitude of 50 mV was used for the contaminated E10 fuel. Then, the polarization curves in the range of 500 mV versus the corrosion potential with a scanning range of 0.3 mV/s were used. The TS measurements were performed from the negative toward the positive potential. For the measurement in the E5 fuel, a Gamry Reference 600 potentiostat was used.^{3,9}

Table 6. Values of the Set Amplitudes for the Individual Fuels in the Three- and Two-Electrode Arrangement

fuel	amplitude (mV)
E85 + 6 vol % H ₂ O	5
E60 + 6 vol % H ₂ O	5
E40 + 2.6 vol % H ₂ O	10
E10 + 0.5 vol % H ₂ O	50
E10 + 0.5 vol % H ₂ O + TBATFB	20, 40 ^a
E5 + 0.25 vol % H ₂ O	50
E5 + 0.25 vol % H ₂ O + TBATFB	30, 50 ^a

^aA higher amplitude was used in the three-electrode arrangements at higher ohmic resistance values.

For the polarization curves, the *iR*-drop compensation was performed by subtracting its value from the measured curves. The ohmic resistance used for the compensation was evaluated from the high-frequency limit of the impedance spectra measured before the polarization measurement.

The Tafel coefficients for the anode (β_a) and cathode (β_c) spectrum parts were obtained by the linear approximation of the Tafel parts of the polarization curves and their subsequent extrapolation. From the Tafel coefficients, polarization resistance (R_p), and electrode surface, the corrosion current density (i_{corr}) was calculated according to the Stern–Geary equation (eq 3).

$$i_{\text{corr}} = \frac{\beta_c \beta_a}{2.3(\beta_c + \beta_a)R_p} \quad (3)$$

4.3.2. Two-Electrode Arrangement (EIS). For the planar, two-electrode arrangement, a Reference 600 potentiostat was used. The measuring electrode system consisted of two planar symmetrically arranged mild steel electrodes of a dimension of 3 × 4 cm. The distance between the electrodes was 1 mm. Both electrodes were, from the external part, embedded into an epoxide resin so that the whole electrode including the edges was isolated from the corrosive environment. The total exposed area of both electrodes was 24 cm². The electrode system was placed in a cell containing 100 mL of a corrosive environment (fuel). The measuring sequence included the OCP stabilization for 24 h. Then, the impedance spectra were measured in the frequency range of 1 MHz to 1 mHz and an amplitude of 20–50 mV. For these high amplitude values, the response linearity was verified.^{3,9}

Before each measurement, the surface of the mild steel electrodes was adjusted by grinding and wet polishing using sandpaper (1200 mesh). Then, the electrode surface was rinsed with demineralized water, degreased with acetone, and

dried with some tissue. This electrode adjustment process was described and demonstrated in detail in our previous paper (Figure 5).³

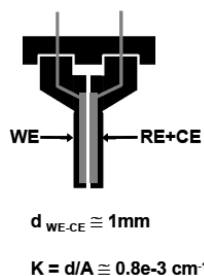


Figure 5. Geometry of a planar, two-electrode arrangement with the distance between the electrodes of about 1 mm, electrode surface area of 12 cm², and a cell constant of about 0.810⁻³ cm⁻¹. Adapted with permission from ref 20. Copyright 2009 Faculty of Environmental Technology, University of Chemistry and Technology Prague.

4.4. Supporting Electrolyte and Addition of the Contaminated E5 and E10 Fuels. Tetrabutylammonium tetrafluoroborate (TBATFB) purchased from Sigma Aldrich (99%, p.a.) was used as a supporting electrolyte to increase the environment (fuel) conductivity. The addition of TBATFB to the contaminated E5 and E10 fuels was performed before the EIS and TS measurements after the corrosion potential was stabilized. The corrosion potential stabilization in the mild steel–fuel (E5, E10) systems with no supporting electrolyte occurred after 23 h. After the stabilization, the TBATFB was added directly into the measuring cell so that the final TBATFB concentration was 500 mg/L. The influence of the TBATFB on the distortion of the measured data was studied in our previous paper.⁹ After the addition of TBATFB to the mild steel–fuel system and its complete dissolution, which occurred within 15 min, the stabilization of the system corrosion potential occurred after 15 min. After this stabilization, the impedance spectra and polarization characteristics were measured. The amplitude at the impedance spectroscopy after the addition of TBATFB was selected depending on the change in fuel conductivity so that the response linearity was maintained (see Table 6). This addition procedure was chosen to minimize the potential negative effects of TBATFB on the distortion of the measured corrosion data due to its adsorption on the steel surface.

EIS measurements in low-conductivity E5 and E10 fuels were performed at high amplitude values (see Table 6) to obtain continuous spectra by avoiding spectra distortion by the response error at individual frequencies. The choice of optimum measuring amplitude is crucial as the output signal can be weak and distorted by noise when the amplitude is insufficient. It is a fact that the lower is the environment (fuel) conductivity and the higher is the distance between the reference and working electrode (i.e., the series ohmic resistance increases), the higher amplitudes are needed for EIS measurements. For instance, significantly noise-distorted spectra were obtained for the tested E5 and E10 fuels at the amplitude of 5 mV. On the contrary, the spectra measured in the sufficiently conductive E40–E85 fuels at high amplitudes (e.g., 50 mV) can be distorted due to the concentration changes on the working electrode surface.³¹ These negative effects need to be prevented by choosing an appropriate amplitude value. For these reasons, it was impossible to

perform the EIS measurements at the same amplitude value over the entire range of the ethanol content in the EGBs.

AUTHOR INFORMATION

Corresponding Author

Martin Staš – Department of Petroleum Technology and Alternative Fuels, University of Chemistry and Technology Prague, 166 28 Prague, The Czech Republic; orcid.org/0000-0002-3106-8601; Email: Martin.Stas@vscht.cz

Authors

Lukáš Matějovský – Department of Petroleum Technology and Alternative Fuels, University of Chemistry and Technology Prague, 166 28 Prague, The Czech Republic; orcid.org/0000-0002-0248-4809

Jan Macák – Department of Power Engineering, University of Chemistry and Technology Prague, 166 28 Prague, The Czech Republic

Complete contact information is available at: <https://pubs.acs.org/10.1021/acsoomega.1c02320>

Notes

The authors declare no competing financial interest.

ACKNOWLEDGMENTS

This research was funded from the institutional support for the long-term conceptual development of the research organization (company registration number CZ60461373) provided by the Ministry of Education, Youth and Sports of the Czech Republic.

ABBREVIATIONS

CE	counter (auxiliary) electrode
CPE	constant phase element
EGBs	ethanol–gasoline blends
EIS	electrochemical impedance spectroscopy
OCP	open circuit potential
RE	reference electrode
TBATFB	tetrabutylammonium tetrafluoroborate
TS	Tafel scan
WE	working electrode

REFERENCES

- (1) REN 21: Renewables 2019—Global Status Report, 2019. <https://www.ren21.net/gsr-2019/> (accessed Oct 24, 2019).
- (2) Ray, R. C.; Ramachandran, S. *Bioethanol Production from Food Crops: Sustainable Sources, Interventions, and Challenges*; Academic Press, 2018.
- (3) Matějovský, L.; Macák, J.; Pleyer, O.; Staš, M. Metal Corrosion and the Efficiency of Corrosion Inhibitors in Less Conductive Media. *J. Visualized Exp.* 2018, 1–16.
- (4) Matějovský, L.; Macák, J.; Pleyer, O.; Straka, P.; Staš, M. Efficiency of Steel Corrosion Inhibitors in an Environment of Ethanol–Gasoline Blends. *ACS Omega* 2019, 4, 8650–8660.
- (5) Baena, L.; Gómez, M.; Calderón, J. Aggressiveness of a 20% Bioethanol–80% Gasoline Mixture on Autoparts: I Behavior of Metallic Materials and Evaluation of Their Electrochemical Properties. *Fuel* 2012, 95, 320–328.
- (6) De Souza, J.; Mattos, O.; Sathler, L.; Takenouti, H. Impedance Measurements of Corroding Mild Steel in an Automotive Fuel Ethanol with and without Inhibitor in a Two and Three Electrode Cell. *Corros. Sci.* 1987, 27, 1351–1364.

- (7) Jahnke, H.; Schönborn, M. Electrochemical Corrosion Measurements in Motor Fuels Based on Methanol and Ethanol. *Mater. Corros.* **1985**, *36*, 561–566.
- (8) Matějovský, L.; Macák, J.; Staš, M. Cyclic Potentiometric Polarization and Resistance of Mild Steel in an Environment of Alcohols and Their Blends with Gasoline. *ACS Omega* **2019**, *4*, 21548–21558.
- (9) Matějovský, L.; Staš, M.; Dumská, K.; Pospíšil, M.; Macák, J. Electrochemical Corrosion Tests in an Environment of Low-Conductive Ethanol-Gasoline Blends: Part 1—Testing of Supporting Electrolytes. *J. Electroanal. Chem.* **2021**, *880*, No. 114879.
- (10) Matějovský, L.; Macák, J.; Pospíšil, M.; Baroš, P.; Staš, M.; Krausová, A. Study of Corrosion of Metallic Materials in Ethanol-Gasoline Blends: Application of Electrochemical Methods. *Energy Fuels* **2017**, *31*, 10880–10889.
- (11) Matějovský, L. S.; Macák, J.; Pospíšil, M.; Staš, M.; Baroš, P.; Krausová, A. Study of Corrosion Effects of Oxidized Ethanol-Gasoline Blends on Metallic Materials. *Energy Fuels* **2018**, *32*, 5145–5156.
- (12) Lou, X.; Singh, P. M. Role of Water, Acetic Acid and Chloride on Corrosion and Pitting Behaviour of Carbon Steel in Fuel-Grade Ethanol. *Corros. Sci.* **2010**, *52*, 2303–2315.
- (13) Lou, X.; Singh, P. M. Cathodic activities of oxygen and hydrogen on carbon steel in simulated fuel-Grade Ethanol. *Electrochim. Acta* **2011**, *56*, 2312–2320.
- (14) Nie, X.; Li, X.; Northwood, D. O. Corrosion Behavior of metallic materials in ethanol-gasoline alternative fuels. *Mater. Sci. Forum* **2007**, *546–549*, 1093–1100.
- (15) Gui, F.; Sridhar, N. Conducting Electrochemical Measurements in Fuel-Grade Ethanol Using Microelectrodes. *Corrosion* **2010**, *66*, No. 045005.
- (16) Cao, L.; Frankel, G.; Sridhar, N. Effect of Chloride on Stress Corrosion Cracking Susceptibility of Carbon Steel in Simulated Fuel Grade Ethanol. *Electrochim. Acta* **2013**, *104*, 255–266.
- (17) Park, I.-J.; Nam, T.-H.; Kim, J.-H.; Kim, J.-G. Evaluation of corrosion characteristics of aluminum alloys in the bio-Ethanol Gasoline Blended Fuel by 2-Electrode Electrochemical Impedance Spectroscopy. *Fuel* **2014**, *126*, 26–31.
- (18) Hoai Vu, N. S.; Hien, P. V.; Mathesh, M.; Hanh Thu, V. T.; Nam, N. D. Improved Corrosion Resistance of Steel in Ethanol Fuel Blend by Titania Nanoparticles and Aganonerion polymorphum Leaf Extract. *ACS Omega* **2019**, *4*, 146–158.
- (19) Carpintero, E. M.; Ramos, I. S.; Rosas, G.; Medina, M. E.; Sarmiento-Bustos, E.; Lopez-Sesenes, R.; Gonzalez-Rodriguez, J. Al-Mg Alloys Prepared by Mechanically Alloying Reinforced with Carbon Nanotubes and Their Corrosion Behavior in Bioethanol. *Int. J. Electrochem. Sci.* **2020**, *15*, 3029–3039.
- (20) Macák, J.; Černoušek, T.; Jiříček, I.; Baroš, P.; Tomášek, J.; Pospíšil, M. Elektrochemické korozní testy v kapalných biopalivech. (Electrochemical Corrosion Tests in Liquid Biofuels, in Czech). *Paliva* **2009**, *1*, 1–4.
- (21) Cao, L.; Frankel, G.; Sridhar, N. Effect of Oxygen on Ethanol Stress Corrosion Cracking Susceptibility: Part 1—Electrochemical Response and Cracking-Susceptible Potential Region. *Corrosion* **2013**, *69*, 768–780.
- (22) Gui, F.; Sridhar, N.; Beavers, J. Localized Corrosion of Carbon Steel and Its Implications on the Mechanism and Inhibition of Stress Corrosion Cracking in Fuel-Grade Ethanol. *Corrosion* **2010**, *66*, No. 125001.
- (23) Lou, X.; Singh, P. M. Phase Angle Analysis for Stress Corrosion Cracking of Carbon Steel in Fuel-Grade Ethanol: Experiments and Simulation. *Electrochim. Acta* **2011**, *56*, 1835–1847.
- (24) Joseph, O. O.; Loto, C. A.; Sivaprasad, S.; Ajayi, J. A.; Tarafder, S. Role of Chloride in the Corrosion and Fracture BEHAVIOR of Micro-Alloyed Steel in E80 Simulated Fuel Grade Ethanol Environment. *Materials* **2016**, *9*, No. 463.
- (25) Samusawa, I.; Shiotani, K. Influence and Role of Ethanol Minor Constituents of Fuel Grade Ethanol on Corrosion Behavior of Carbon Steel. *Corros. Sci.* **2015**, *90*, 266–275.
- (26) Vu, N.; Hien, P.; Man, T.; Hanh Thu, V.; Tri, M.; Nam, N. A Study on Corrosion Inhibitor for Mild Steel in Ethanol Fuel Blend. *Materials* **2018**, *11*, No. 59.
- (27) Eppel, K.; Scholz, M.; Troßmann, T.; Berger, C. Corrosion of Metals for Automotive Applications in Ethanol Blended Biofuels. *Energy Mater.* **2008**, *3*, 227–231.
- (28) Joseph, O. O.; Ajayi, J. A. Data on Chloride-Related Electrochemical Deterioration of Micro-Alloyed Steel in E20 Simulated Fuel Ethanol Blend. *Chem. Data Collect.* **2020**, *27*, No. 100384.
- (29) Sridhar, N.; Price, K.; Buckingham, J.; Dante, J. Stress Corrosion Cracking of Carbon Steel in Ethanol. *Corrosion* **2006**, *62*, 687–702.
- (30) Cao, L.; Frankel, G.; Sridhar, N. Supporting Electrolyte for Corrosion and Cracking Studies in Deaerated Simulated Fuel Grade Ethanol. *J. Electrochem. Soc.* **2013**, *160*, C19–C27.
- (31) Macdonald, J. R.; Johnson, W. B. Fundamentals of impedance spectroscopy. In *Impedance Spectroscopy: Theory, Experiment, and Applications*, 3rd ed.; Barsoukov, E.; Macdonald, J. R., Eds.; John Wiley & Sons, Inc., 2018; pp 1–20.